Journal of Materials Chemistry

Cite this: DOI: 10.1039/c2jm30944k

www.rsc.org/materials

PAPER

Exploiting the localized surface plasmon modes in gold triangular nanoparticles for sensing applications

Rodica Morarescu,*[a] Honghui Shen,[b] Renaud A. L. Vallée,[c] Bjorn Maes,[bd] Branko Kolaric[a] and Pascal Damman[a]

Received 15th February 2012, Accepted 20th April 2012
DOI: 10.1039/c2jm30944k

In this study we investigate and exploit, for optical sensing, the surface plasmon excitation in gold triangular nanoparticles with high aspect ratios (*i.e.*, the ratio of the edge length of the triangles with the height) prepared by nanosphere lithography. As shown previously, the shape and size of these nanoparticles were used to tune their optical properties, monitored by far field extinction spectroscopy. Interestingly, several localized surface plasmon resonances were detected in the visible and near infrared regions and were attributed to dipole and quadrupole modes. These modes, identified from numerical simulations, "red-shift" as the aspect ratio of the particles increases. The plasmon modes observed for larger triangles exhibit unexpected sensitivity with a change in the refractive index. From experiments and numerical simulations, this higher sensitivity has been attributed to an increase of the local field enhancement for sharper tips. This new effect can provide important information for the design of particles as building blocks for sensing applications.

I. Introduction

Plasmonic nanostructures have received increasing attention in recent decades due to their unique optical properties. These properties are dominated by localized surface plasmon polariton resonances (LSPPRs), *i.e.* collective oscillations of the conduction band electrons, driven by an incident electromagnetic field. The frequency, width and amplitude of these resonances strongly depend on the morphology of the nanoparticles (NPs), in particular on their size and shape, and on the dielectric function of the surrounding medium. The collective oscillation of the conduction band electrons is accompanied by an enhancement of the local field in the vicinity of the NP's surface. Various chemical and biological applications take advantage of the high sensitivity of LSPPRs to the refractive index of the medium in the vicinity of the metal surface. Small changes in the local refractive index yield spectral shifts of the LSPPR peak observed in the extinction spectra. This shift in wavelength per unit change in the refractive index (RIU) of the surrounding medium is used to quantify the sensitivity factor S of the NPs.

There is a permanent interest to develop and to improve the sensitivity of optical sensors based on metal NPs.[1,2] A variety of chemical syntheses and lithographic techniques have opened possibilities to design new plasmonic structures with defined sizes and shapes, dispersed in solutions or supported on substrates. In particular, arrays of supported monodisperse NPs represent potential structures for many applications such as optical sensing,[3] surface enhanced Raman scattering (SERS),[4–6] surface-enhanced fluorescence microscopy,[7] nanopatterning[8,9] and solar cells.[10,11] Conventional lithography techniques, such as electron beam lithography (EBL)[12,13] and focused ion beam lithography (FIB),[14] can routinely fabricate ordered arrays of metal NPs. Besides these standard techniques, new methods taking advantage of the self-assembly of colloids (nanosphere lithography, NSL)[15] were developed to produce regular arrays of gold NPs. The main advantage of this powerful technique is the low-cost fabrication of large arrays of NPs with controlled size, shape and interparticle distance. NP arrays prepared by NSL have been extensively studied in recent years. For instance, Jensen *et al.* demonstrated the ability of NSL to tune the optical properties of triangular NPs across the visible and near IR region.[16]

Although many studies have been reported, a detailed investigation of triangular NPs with very high aspect ratios (AR, *i.e.* ratio of the edge length and height) is still missing. The aim of the present work is to investigate the optical properties of such gold triangular NPs prepared by NSL with AR ranging between 2.7 and 7.2. The extinction spectra of these NP arrays reveal the presence of two intense plasmon resonances that were attributed to dipole and quadrupole modes spectrally resolved in the visible and IR region. In addition, increasing the AR produces a gradual

[a]*Laboratoire Interfaces & Fluides Complexes, Centre d' Innovation et de Recherche en Matériaux Polymères, Université de Mons, 20 Place du Parc, B-7000 Mons, Belgium. E-mail: rodica.morarescu@umons.ac.be*
[b]*Photonics Research Group (INTEC), Ghent University-Imec, Sint-Pietersnieuwstraat 41, B-9000 Ghent, Belgium*
[c]*Centre de Recherche Paul Pascal (CNRS-UPR8641), 115 avenue du docteur Schweitzer, 33600 Pessac, France*
[d]*Micro- and Nanophotonic Materials Group, Faculty of Science, University of Mons, 20 Place du Parc, B-7000 Mons, Belgium*

red-shift of the LSPPRs that drastically improves the spectral resolution of the modes. Finally we demonstrate that these larger NPs are superior candidates for (bio)sensing applications thanks to their very high sensitivity to change in the refractive index of the surrounding medium. This higher sensitivity was associated with the stronger local field enhancement reached in the vicinity of the sharp tips of the larger NPs.

II. Experimental techniques

As mentioned above, the experiments presented here use arrays of triangular gold NPs prepared by NSL,[18] utilizing the drop coating method of Micheletto *et al.*[19] The technique employs nanospheres dispersed in solution to create a close-packed monolayer with hexagonal symmetry, used as a mask in a subsequent step, where gold is deposited through the nanospheres to fill the void spaces in the layer lattice. In this way regular arrays of triangular gold NPs are fabricated in a last step, when the nanosphere mask is removed. NSL has the advantage of making it possible to largely tune the AR of the NPs by changing the size of the nanospheres used as a mask and/or by changing the thickness of the evaporated gold. In this contribution monolayers of nanospheres with a diameter D of 356 nm, 456 nm, 628 nm and 771 nm have been prepared on fused silica substrates and used as a lithographic mask in a subsequent step when gold was evaporated. The gold film thickness determined by a quartz crystal microbalance was fixed to 40 nm. After the nanosphere masks are removed triangular NP arrays with the following edge length remain on the substrates: $l = 109$ nm, 135 nm, 180 nm and 288 nm. The aspect ratio of these NPs increases linearly with the edge length as follows: 2.7 (array $AR_{2.7}$), 3.4 (array $AR_{3.4}$), 4.5 (array $AR_{4.5}$) and 7.2 (array $AR_{7.2}$).

The AR of the NPs can also be tuned by changing the thickness of the evaporated gold for a constant nanosphere diameter. For example, in this context, for the NPs designed using nanospheres with diameter $D = 771$ nm, 80 nm of gold was evaporated in a second step instead of 40 nm. As a consequence, the AR of the NPs was changed from 7.2 (array $AR_{7.2}$) to 3.6 (array $AR^{*}_{3.6}$).

The samples have been characterized by atomic force microscopy (AFM) and the edge length values of the NPs presented above have not been deconvoluted for tip broadening effects. In order to monitor the optical properties of triangular NPs, far field visible-near infrared (NIR) extinction spectroscopy in the wavelength range 400–1800 nm has been applied. All the extinction spectra here presented are recorded using unpolarized light, under normal incidence with respect to the sample surface. In order to probe the sensitivity of the NPs the extinction spectra were recorded when the samples were placed in different environments with a different refractive index.

III. Results and discussion

A. Investigation of multipolar plasmon modes

Fig. 1 shows the AFM images of the different highly ordered triangular NPs used in this study. The experimental extinction spectra of these arrays are presented in Fig. 2a.

For array $AR_{2.7}$ the dominant resonance is an extinction band at 851 nm. Additionally a weaker band arises at 609 nm. Increasing the AR at constant gold thickness leads to a gradual red-shift of these resonances from array $AR_{2.7}$ to array $AR_{7.2}$. For example, for array $AR_{7.2}$ the strong and weak bands are located at 1463 nm and 730 nm, respectively. As the AR of the triangles increases, we also observe an increase in their intensity, bandwidth and a better separation of both LSPPRs.

Changing the gold thickness also affects the optical properties of the NP array. Fig. 3 shows that the dipole resonance experienced a 440 nm blue-shift from array $AR_{7.2}$ to array $AR^{*}_{3.6}$ (same edge length but different height, 40 and 80 nm, respectively). Additionally a narrowing of plasmon width has been observed due to the decrease of the AR.

To have a better insight into the optical properties of these triangular NPs we simulate the extinction spectra of the NPs arrays by finite-element COMSOL simulations. This method has been extensively used for plasmonic simulations, see *e.g.* ref. 20. Fig. 4 depicts the schematic representation of the triangular NP's geometry used in the simulations: (a) perspective view and (b) top view. The symmetry of the lattice and the perpendicular excitation allows the use of only one cell as depicted in Fig. 4, with the use of appropriate boundary conditions. Numerical extinction is determined by calculating $1 - T$, with T the normalized transmitted power through a plane underneath the particles. For gold we used index data from Palik,[21] for the substrate index we employed $n = 1.5426$.

The polarization direction has been chosen along the bisector of the triangular NPs. Only the in plane excitation has been investigated. The sharpness of the tips has been controlled by adjusting the angle θ ($\theta = 2L/D$ is a geometrical parameter without dimension describing the sharpness of the tip, see Fig. 4). A decrease of θ is obviously related to an increase of tip sharpness. Please note that care has to be given to the geometric parameters used to model the experiments, in order to fall well within the range of the experimentally measured values. For each specific NP array geometry, the θ angle was adjusted to have a good agreement with the experimental extinction spectra. For the NP arrays $AR_{2.7}$, $AR_{3.4}$ and $AR_{4.5}$, we used θ values of 0.49 (28°), 0.49 (28°) and 0.42 (24°), respectively. The largest NPs ($AR_{4.5}$, edge length 180 nm) have thus the sharpest tips (smallest θ).

The simulated extinction spectra of triangular NP arrays $AR_{2.7}$, $AR_{3.4}$ and $AR_{4.5}$ are given in Fig. 2b. Similar trends as in the experimental spectra are observed: (i) the presence of two significant resonances, (ii) these resonances are gradually red-shifted and (iii) their bandwidth increases with the increasing edge length of the triangles. Additionally for array $AR_{4.5}$, besides the two main resonances, multiple weak higher-order peaks show up at around 670 nm.

Interestingly, the experimental spectra can be adequately reproduced with a single "fitting" parameter, the θ angle. For all arrays, the position of the maximum LSPPR for the fundamental resonance ($l = 1$) of the calculated spectra matches well with the experimental ones within ±20 nm. For the second order LSPPR ($l = 2$), the calculated peaks are slightly red-shifted compared to the experimental ones. Nevertheless, it should be noted that in the calculations these resonances appear to be slightly split into two modes. A slight blue-shift can be observed in the experimental spectra due to a possible overlapping of the peaks and experimental broadening. We assign the fundamental sharp resonance to the dipolar mode and the second order resonance

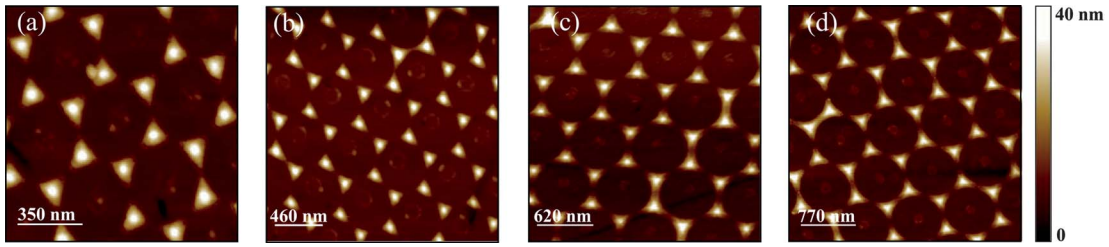

Fig. 1 AFM images of triangular NP arrays with various ARs, (a) $AR_{2.7}$, (b) $AR_{3.4}$, (c) $AR_{4.5}$ and (d) $AR_{7.2}$. See text for details about these arrays.

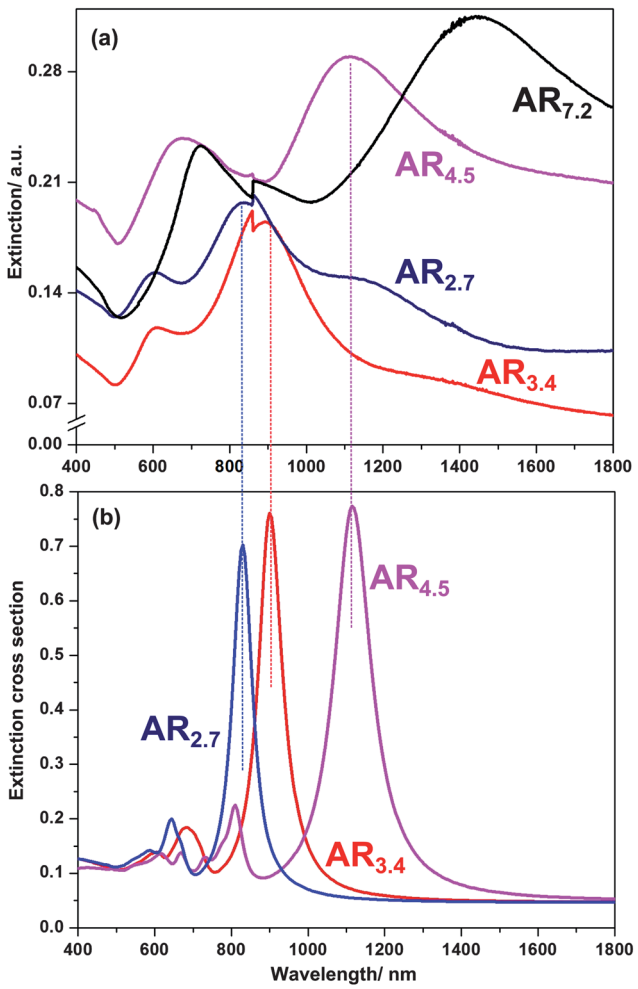

Fig. 2 (a) *Experimental* extinction spectra of NP arrays with different aspect ratios $AR_{2.7}$, $AR_{3.4}$, $AR_{4.5}$ and $AR_{7.2}$, as indicated. The spectra were recorded under normal incidence using unpolarized light. (b) *Simulated* extinction spectra of triangular NP arrays $AR_{2.7}$, $AR_{3.4}$ and $AR_{4.5}$.

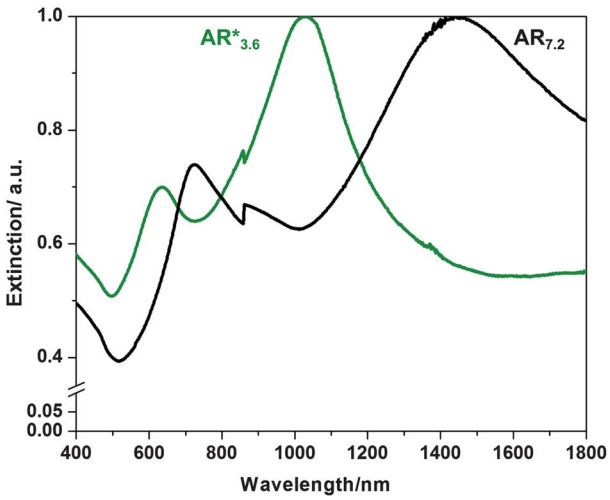

Fig. 3 Experimental extinction spectra of NP arrays prepared using the same diameter of the nanospheres $D = 771$ nm but different gold thickness: 40 nm ($AR_{7.2}$) and 80 nm ($AR^{*}_{3.6}$).

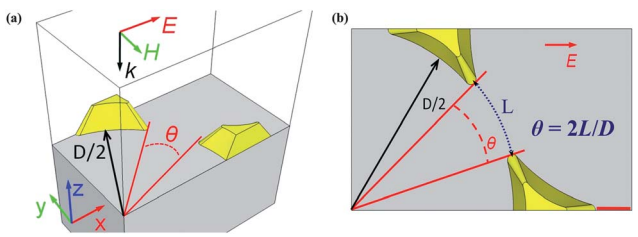

Fig. 4 Schematic representation of a triangular NP's geometry as used in COMSOL simulations: (a) perspective view and (b) top view respectively. The sharpness of the tips has been controlled by adjusting the angle (θ).

observed for the shorter wavelengths to the quadrupole mode. For array $AR_{4.5}$ a weak resonance is observed at 670 nm in the simulated spectra that may be attributed to the excitation of multipolar modes higher than $l = 2$. The experimental peaks are broader than the numerical ones, which can be attributed to deviations from perfect periodicity (*e.g.* size inhomogeneity) in the experimental samples.

Fig. 5 reveals the linear dependence of the experimentally determined wavelengths corresponding to the maximum extinction bands of the dipole and quadrupole modes *versus* the aspect ratios, as expected for such triangular NP arrays.[25]

Besides the far field properties, the near field optical properties of the triangular NP arrays $AR_{2.7}$, $AR_{3.4}$ and $AR_{4.5}$ have been numerically investigated. Fig. 6 shows the calculated electric field maps close to the particle surface of array $AR_{4.5}$ for the LSPPRs attributed to the dipole ($\lambda = 1115$ nm (a)) and quadrupole ($\lambda = 810$ nm (b)) excitations. These electric field maps correspond to NP arrays supported on a fused silica substrate and a polarization direction along the bisector of the triangles. For the dipole and quadrupolar resonances, the largest fields are generated on the NPs tips that are aligned with the polarization direction (see Fig. 6a and b). Negligible field

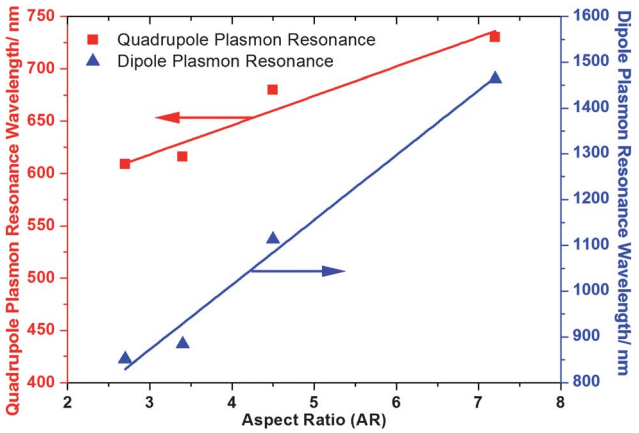

Fig. 5 The linear relationship between the experimental LSPPR wavelengths of the dipole (blue) and quadrupole (red) *vs.* the aspect ratios of the gold nanotriangles. All the extinction spectra have been recorded in air. The axes are as indicated.

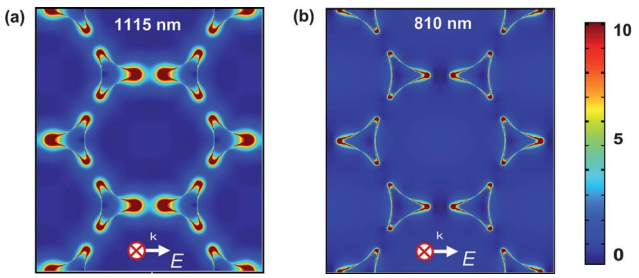

Fig. 6 2D maps representing the square of the electric field external to triangular gold NP array $AR_{4.5}$. The sharpness of the NPs has been chosen by fixing the angle θ at 24°. The polarization of light is along the triangle's bisector. The map has been calculated for the LSPPRs which correspond to the dipole resonance $\lambda = 1115$ nm (a) and quadrupolar resonance $\lambda = 810$ nm (b).

enhancements can be observed for the tips perpendicular to the polarization direction.

It is well known that the optical properties of metal NPs are influenced by *particle size*. With increasing particle size higher order plasmon modes appear in the extinction spectrum.[23] These results can be explained by considering that for larger NPs, the incoming light cannot polarize the particle homogeneously. As a consequence, retardation effects lead to a gradient of the electromagnetic field, that excite higher order modes. A broadening of the plasmon bandwidth is observed for large NPs as a result of radiative damping. The retardation effects within the particles lead to a considerable decrease in the plasmon lifetime and thus the dipolar near field enhancement.

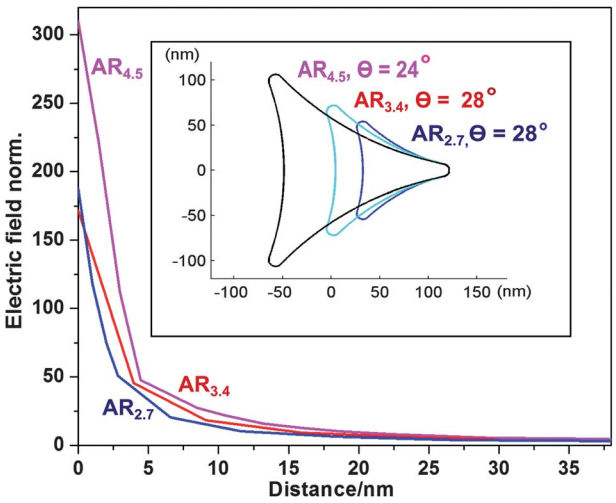

Fig. 8 Electric field normalized (dipole excitation) for NP arrays $AR_{2.7}$, $AR_{3.4}$ and $AR_{4.5}$. The sharpness of the tips was adjusted to reproduce the experimental spectra. The inset shows the shapes of the triangles with different sharpness used in the COMSOL simulations.

The optical properties of metal NPs are also strongly influenced by *particle shape*. This effect is obvious for very different geometries such as spheres, rods, squares and triangles. In a more subtle way, it has been shown recently by Sherry *et al.* that the sharpness of the tips of the triangular NPs affects their optical properties drastically.[17] The drastic influence of the *snipping effect* (*i.e.* rounding of the tips) on the optical properties of triangular NPs has been concomitantly reported.[22,24]

For the design of NPs and the tuning of their optical properties, both size and shape are thus of a crucial importance. For NP

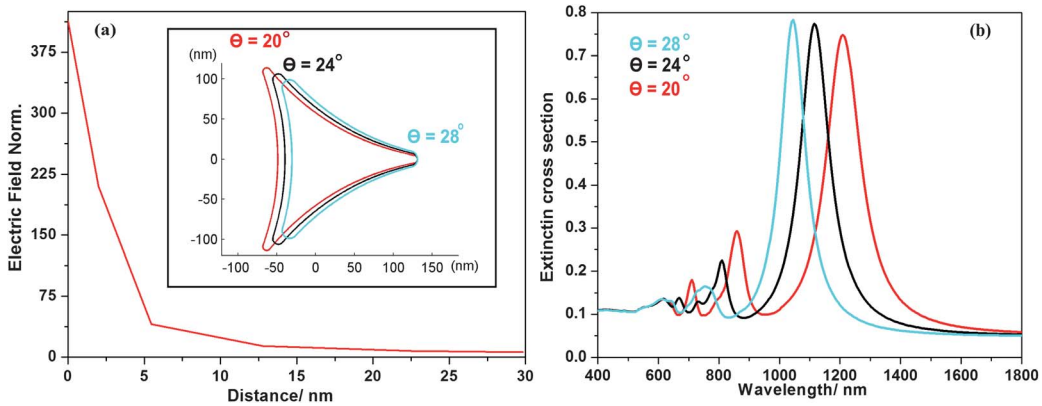

Fig. 7 (a) The evolution of the normalized electric field with distance from the tip for a triangular NP array $AR_{4.5}$ and an angle θ equal to 20°. The electric field corresponds to the dipolar mode. The inset shows the shapes of the triangles with different sharpness used in the simulations θ: 20°, 24°, 28°. (b) The evolution of the extinction spectra of similar triangular NPs with various θ angles, as indicated.

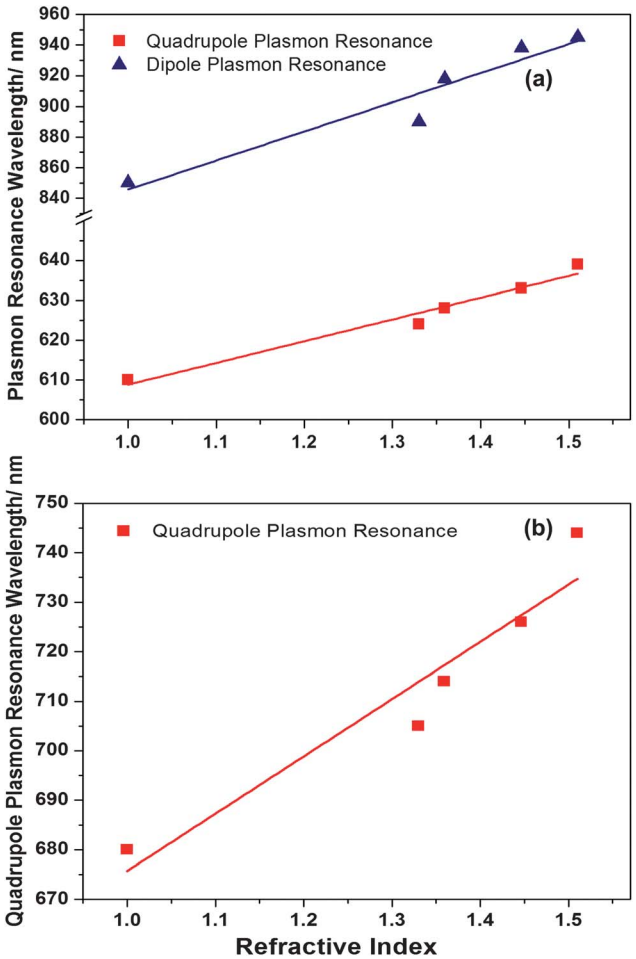

Fig. 9 (a) The linear relationship between the experimental LSPPR wavelengths of the dipole (blue) and quadrupole (red) of the NP array $AR_{2.7}$ *vs.* the refractive index of different solvents. (b) The linear relationship between the experimental LSPPR wavelengths of the quadrupole (red) of the NP array $AR_{4.5}$ *vs.* the surrounding refractive index.

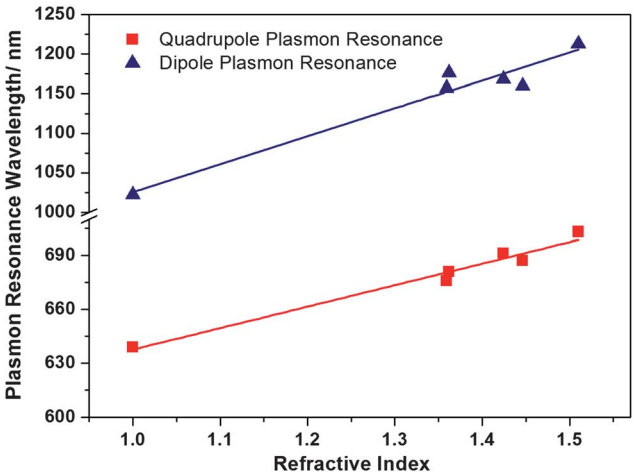

Fig. 10 The evolution of the experimental LSPPR wavelengths of the dipole (blue) and quadrupole (red) resonance for the NP array $AR^{*}_{3.6}$ with the refractive indexes of different surrounding solvents.

arrays prepared by NSL, the sharpness of the tips is clearly affected by a change of the colloidal sphere's diameter (see Fig. 1 and 2). The influence of the tip sharpness (determined by the angle θ) was investigated with COMSOL simulations.

Fig. 7a depicts the rapid decrease of the electric field with the distance from the tip, for the dipole mode of NP array $AR_{4.5}$. From the extinction spectra of these NPs (Fig. 7b), we see that the dipole resonance is very sensitive to the tip sharpness, red-shifts as large as 170 nm are observed for the sharpest triangles ($\theta = 20°$).

The dramatic effect of the tip sharpness on the optical spectra of the NPs can be explained by taking into account that the sharp tips on a perfect triangle lead to polarization distortions that favor higher order multipoles.[25] For snipped triangular NPs, this effect is reduced and the electric field becomes more homogeneous.

B. Optical sensing based on the exploitation of plasmon modes in triangular NPs

As shown in Fig. 8, the sizes of the triangular NPs affect the field enhancement near the tip. From COMSOL simulations, we can see that the field decays away from the tip surface faster for smaller NPs. If we consider that a higher enhancement of the near fields correlates with a higher sensitivity, then we can conclude that the largest NPs with sharper tips are excellent candidates for sensing applications.

In the following, we demonstrate experimentally that the largest NPs are the most sensitive. Shifts in the LSPPR peak position for dipole and quadrupole resonances are observed by changing the refractive index of the surrounding solvent (Fig. 9). This gives us the opportunity to measure the sensitivity (given by the wavelength shift per RIU) for the NP arrays $AR_{2.7}$, $AR_{3.4}$ and $AR_{4.5}$.

Fig. 9a shows the evolution of the LSPPR peak position (dipole and quadrupole) for NP array $AR_{2.7}$ with the surrounding refractive index. From these data, sensitivity factors of 190 nm per RIU for the dipole and 54 nm per RIU for the quadrupole are obtained. For the NP array $AR_{4.5}$, only the sensitivity of the quadrupole resonance (116 nm per RIU) was determined (see Fig. 9b). Due to the near-IR absorption of the solvents used for tuning the refractive index, it was not possible to record the LSPPR shift of the dipole mode.

However, the shift observed for the dipole resonance of the array of largest particles $AR_{4.5}$ immersed in pyridine is two times larger than those observed for the array of smallest particles $AR_{2.7}$ immersed in the same solvent.

For the studied NP arrays, the dipole resonance is more sensitive to a change in the refractive index compared to the quadrupole resonance. The sensitivity of the triangular NPs clearly increases with increasing their edge length at constant gold thickness.

To further support this observation and avoid the near-IR absorption of solvent, the sensitivity of large particles, $D = 771$ nm with a gold thickness of 80 nm (array $AR^{*}_{3.6}$) has been investigated. The resulting sensitivity will be a lower bound of the value expected for the 40 nm array $AR_{7.2}$. Indeed, Haes *et al.* reported that triangular NPs with the smallest thickness are the most sensitive.[26]

For the NP array $AR^{*}_{3.6}$, very large sensitivity factors of 353 nm per RIU and 120 nm per RIU were measured for the dipole and quadrupole resonance (Fig. 10).

We have demonstrated that triangular NP arrays designed with the largest colloidal nanospheres (largest edge length) and smallest gold thickness are the most sensitive and the best candidates for the design of (bio)sensors in the near-infrared region.

IV. Conclusions

In this study, the optical properties of large triangular NPs prepared by nanosphere lithography have been investigated. We have shown that besides the dipole mode, multipolar plasmon modes are excited in these NP arrays. The dipole and quadrupole modes, as identified by COMSOL simulations, red-shift as the edge length of the triangles increases for a given gold thickness. These resonances are well resolved allowing us to investigate them individually in the context of sensing applications. Additionally we found that by increasing the edge length of the triangles the tips of the NPs became sharper and in this way a larger amplification of the near field was reached on the sharpest tips. As a consequence NPs prepared with larger colloidal nanospheres are better candidates for sensing applications due to their high sensitivity factors. These results open the way to the new design of plasmonic structures as building blocks for sensing applications.

Acknowledgements

R.M. and P.D. acknowledge the financial support from the EU-FEDER and Interreg IV, project PlasmoBio. B.K. acknowledges the financial support from Smart film grant 830039 (ECV12020020892F) in the framework of the Convergence Project. R.M., P.D., and B.K. acknowledge the financial support from FRS-FNRS. H.S. and B.M. acknowledge the financial support by the IWT *via* the SBO-project no. 060843 "Polyspec", by the Interuniversity Attraction Poles program of the Belspo grant no. IAP P6-10 "photonics@be" and by COST action MP0702. R.V. acknowledges FRS-FNRS for a visiting professor grant. All authors warmly acknowledge Prof. Koen Clays (KU Leuven) for providing the setup for the optical measurements.

References

1 M. A. Mahmoud and M. A. El-Sayed, *J. Am. Chem. Soc.*, 2010, **132**, 12704–12710.
2 J. N. Anker, W. P. Hall, O. Lyandres, N. C. Shah, J. Zhao and R. P. Van Duyne, *Nat. Mater.*, 2008, **7**, 442.
3 S. Enoch, R. Quidant and G. Badenes, *Opt. Express*, 2004, **12**, 3422.
4 J. Z. Zhang and C. Noguez, *Plasmonics*, 2008, **3**, 127.
5 P. L. Stiles, J. A. Dieringer, N. C. Shah and R. P. Van Duyne, *Annu. Rev. Anal. Chem.*, 2008, **1**, 601.
6 B. C. Galarreta, P. R. Norton and F. L. Labarthet, *Langmuir*, 2011, **27**(4), 1494.
7 M. Alschinger, M. Maniak, F. Stietz, T. Vartanyan and F. Träger, *Appl. Phys. B: Lasers Opt.*, 2003, **76**, 771.
8 F. Hubenthal, R. Morarescu, L. Englert, L. Haag, T. Baumert and F. Träger, *Appl. Phys. Lett.*, 2009, **95**, 063101.
9 R. Morarescu, L. Englert, B. Kolaric, P. Damman, R. A. L. Vallée, T. Baumert, F. Hubenthal and F. Träger, *J. Mater. Chem.*, 2011, **21**, 4076.
10 A. Abass, H. Shen, P. Bienstman and B. Maes, *J. Appl. Phys.*, 2011, **109**, 023111.
11 H. Shen, P. Bienstman and B. Maes, *J. Appl. Phys.*, 2009, **106**(7), 073109.
12 T. Ito and S. Okazaki, *Nature*, 2000, **406**, 1027.
13 H. Duan, J. Zhao, Y. Zhang, E. Xie and L. Hanhh, *Nanotechnology*, 2009, **20**, 135306.
14 N. Puttaraksa, S. Gorelick, T. Sajavaara, M. Laitinen, S. Singkarat and H. J. Whitlow, *J. Vac. Sci. Technol., B*, 2008, **26**, 1732.
15 C. L. Haynes and R. P. Van Duyne, *J. Phys. Chem. B*, 2001, **105**, 5599.
16 T. R. Jensen, M. D. Malinsky, C. L. Haynes and R. P. Van Duyne, *J. Phys. Chem. B*, 2000, **104**, 10549.
17 L. J. Sherry, R. Jin, C. A. Mirkin, G. C. Schatz and R. P. Van Duyne, *Nano Lett.*, 2006, **6**, 2060.
18 C. JohnHulteen and R. P. Van Duyne, *J. Vac. Sci. Technol., A*, 1995, **13**(3), 07342101.
19 R. Micheletto, H. Fukuda and M. Ohtsu, *Langmuir*, 1995, **11**, 3333.
20 S. H. Lim, W. Mar, P. Matheu, D. Derkacs and E. T. Yu, *J. Appl. Phys.*, 2007, **101**, 104309.
21 E. D. Palik, *Handbook of Optical Constants of Solids*, Academic Press, New York, 1985.
22 K. L. Kelly, E. Coronado, L. L. Zhao and G. C. Schatz, *J. Phys. Chem. B*, 2003, **107**, 668.
23 P. Yang, H. Portalès and M. P. Pileni, *J. Phys. Chem. C*, 2009, **113**, 11597.
24 R. Morarescu, D. B. Sánchez, N. Borg, T. A. Vartanyan, F. Träger and F. Hubenthal, *Appl. Surf. Sci.*, 2009, **255**, 9822.
25 K. L. Shuford, M. A. Ratner and G. C. Schatz, *J. Chem. Phys.*, 2005, **123**, 114713.
26 A. J. Haes, S. Zou, G. C. Schatz and R. P. Van Duyne, *J. Phys. Chem. B*, 2004, **108**, 109.

